DETECTION OF STATOR FAULT IN SYNCHRONOUS GENERATOR WITHOUT THE KNOWLEDGE OF THE HEALTHY STATE

M. Irhoumah[1,2], R. Pusca[1], E. Lefevre[2], D. Mercier[2], R. Romary[1]

(1). Univ. Artois, EA 4025 LSEE, F-62400, Béthune, France
(2) Univ. Artois, EA 3926 LGI2A, F-62400, Béthune, France
e-mail: raphael.romary@univ-artois.fr

Abstract – This paper focuses on the detection of inter-turn short circuits which can appear in the stator windings of a salient pole synchronous generator. A diagnosis method based on two external flux sensors is developed. In faulty case, it is shown that variations of reactive power leads to specific variation of sensitive spectral lines in the signals delivered by both sensors. This property allows one to define a diagnostic procedure which does not require the knowledge of the healthy state.

Keywords – Synchronous generator, inter-turn short circuits, magnetic field, diagnostic, stator windings, spectral analysis.

.

INTRODUCTION

The detection of faults in electrical machines has been widely investigated, using different techniques, such as those based on vibrations [1] or current signature analysis [2-4]. On the other hand, methods based on the analysis of external magnetic field have been developed in the 70's [5]. Their main advantages are the non-invasive investigation and the simplicity of implementation. The drawback of these methods is tied to the difficulty for modelling the magnetic field that strongly depends on the electromagnetic behaviour of the stator yoke and of the motor housing, which have an important shielding effect.

However, it has been shown that the external magnetic field is very sensitive to internal fault in the machine [6], and generally, this variable is more sensitive than classical electrical variables because it can detect directly the magnetic imbalance caused by the fault [7,8]. Moreover, fault detection with external magnetic field can be improved by using several sensors placed around the machine. Recently, a method based on two sensors positioned at 180 degrees with respect to each other has been developed [9]. This method analyses the behaviours of the sensitive harmonics measured by each sensor when the load varies in order to detect a stator short-circuit fault. The main advantage of this method is that it does not require the knowledge of the healthy state because the decision is not tied to a comparison with a healthy signature.

The aim of this paper is to investigate the implementation of the method presented in [9] in the case of a synchronous generator connected to the grid. Here the diagnosis method is based on the analysis of sensitive harmonics when the reactive power varies. The paper presents first the modelling of the machine with a stator short cicruit using an analytical approach. Then, the effect of operating condition variation is analyzed. Finally, experimental results are presented.

1. ANALYTICAL MODELLING

The analytical developments concern a three phase, p pole pair salient pole synchronous machine with N^s stator slots. All the q phase coils are series connected (q=1, 2 or 3), each phase is composed of n^s turns per pole pair. The stator is supplied by a three phase balanced sinusoidal voltage system of ω angular frequency (frequency f).

1.1. AIRGAP PERMEANCE

It will be considered that the rotor saliency of the synchronous machine is similar to the rotor slot effect of an induction machine regardless of the rotor structure. The secondary slotting effect due to the dampers, which can possibly exist, will be neglected. Consequently, as the number of rotor saliencies is equal to the pole number of the machine (Fig. 1), the airgap permeance λ can be defined as following [7]:

$$\lambda = \sum_{ks=-\infty}^{+\infty} \sum_{kr=-\infty}^{+\infty} \Lambda_{kskr} \cos\left[\left(ksN^s + 2kr\right)p\alpha^s - 2krp\theta\right]$$

Λ_{kskr} is a permeance coefficient that depends on the slot and the pole geometry. ks and kr are positive, negative or null integers. α^s is the angular abscissa of any point in the air-gap related to the stator referential d^s, tied to the phase 1 axis. θ represents the angular position of the rotor tooth 1 axis relatively to d^s. θ can be expressed as: $\theta = \omega t/p + \theta_0$

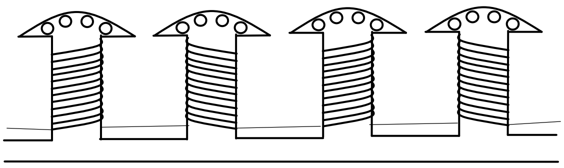

Fig. 1 – Rotor poles

1.2. Stator magneto-motive force

The mmf ε^s generated by the stator of a healthy machine relatively to d^s can be expressed as:

$$\varepsilon^S = I^S \sum_{h^S} A_{h^S} \cos(\omega t - h^S p \alpha^S)$$

h^s takes all the values defined by: $h^s = 6k+1$ where k varies between $-\infty$ to $+\infty$. $A^s_{h^s}$ is a function that takes into account the winding coefficient tied to the rank h^s.

1.3. Airgap flux density

The airgap flux density b^s generated by the stator is obtained by multiplying the ε^s air-gap magnetomotive force (mmf) generated by the stator winding by the λ per area unit air-gap permeance which takes the slotting effect into account. It is shown that the air-gap flux density can be expressed as follows:

$$b^S = \sum_{K,H} b_{K,H}$$

with $b_{K,H} = \hat{b}_{K,H} \cos\left(K\omega t - H\alpha^S - \varphi_{K,H}\right)$

Where K is the frequency rank and H is the pole pair number of a flux density component.

For a healthy machine K and H are defined as:

$$\left.\begin{aligned} K &= 1 + 2kr \\ H &= p(h^S + ksN^S + 2kr \end{aligned}\right\} \qquad (1)$$

1.4. Transverse field

The external magnetic field results from the combination of its axial and transverse components obtained from leakage flux created by the different elements of the machine. The axial field is in a plan that contains the machine axis. It is generated by the winding overhang effects. The transverse field is located in a perpendicular plan to the machine axis. It is an image of the air-gap flux density *b* which is attenuated by the stator magnetic circuit.

In the analytical model, only the transverse field will be considered and particularly its normal component, that requires to define an attenuation coefficient that affect a $b_{K,H}$ component. A simplified geometry of the machine with smooth air-gap used in the analytical model is shown in Fig.2 where the main geometrical parameters are presented

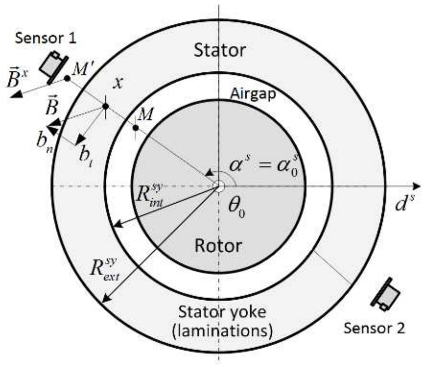

Fig. 2. Simplified geometry of the machine

The attenuation coefficient related to the stator yoke, denoted by C_H, depends on the inner and outer radius of the stator laminations, respectively R^s_{int} and R^s_{ext}, and the magnetic permeability μr [10]. It has been shown that C_H, can be expressed as:

$$C_H = \frac{2}{\mu r \left((R^s_{\text{int}} / R^s_{ext})^{-|H|-1} - (R^s_{\text{int}} / R^s_{ext})^{|H|-1} \right)}$$

Fig. 3 shows the evolution of C_H versus H for $R^s_{\text{int}} = 82.5mm$, $R^s_{ext} = 121mm$ and $\mu r = 1000$. One can observe that the more H increases, the more the components are attenuated.

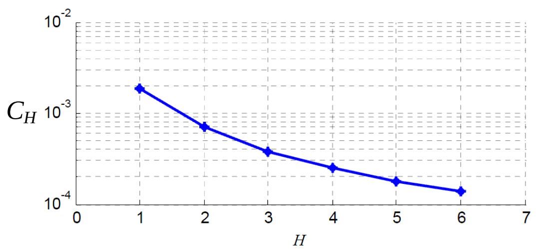

Fig. 3. C_H versus H

1.5. Measurement of the transverse field

As shown in Fig. 2, the measurement is performed with a wound flux sensor placed very closed to the stator core so that only the C_H attenuation coefficient will be considered. Let us denote b^x the normal transverse flux density at radius x= R^s_{ext} . b^x is defined as :

$$b^x = \sum_{K,H} C_H \hat{b}_{K,H} \cos\,(K\omega t - H\alpha^s - \varphi_{K,H}) \quad (10)$$

Let us introduce b^x_K the harmonic of K rank of b^x at the given point M' (x= R^s_{ext} , $\alpha^s = \alpha^s_0$), corresponding to the centre of the wound flux sensor. b^x_K can be defined by:

$$b^x_K = \hat{b}^x_K \cos\,(K\omega t - \varphi^x_K) \quad (11)$$

$\hat{b}^x_K$ can be computed by introducing complex quantities:

$$\hat{b}^x_K = \left| \sum_H C_H \hat{b}_{K,H} e^{-j(H\alpha^s_0 + \varphi_{K,H})} \right| \quad (12)$$

At given α^s_0 , the resulting flux density harmonic at $K\omega$ angular frequency is composed of several elementary components of different polarity *H*.

2. FAULTY MACHINE MODELLING

2.1. SHORT CIRCUIT MODELLING

In order to determine the influence of the faulty turns in the change of the flux density, a model that considers a three-phase stator winding has been developed. In this model, it is supposed that y turns from the n'^s turns of an elementary section belonging to the phase q are short-circuited and that y is small compared with pn^s, the total number of turns per phase. Therefore, it can be assumed that the current remains unchanged and has the same values in each phase in the faulty case. This hypothesis can therefore characterizes the short circuit thanks to a model that preserves the original structure of the machine. This model assumes that the stator winding in presence of the fault is equivalent to the healthy winding, associated to y independent turns in which the short-circuit current circulates. It will be assumed that these two circuits have independent running. The healthy part of the winding generates therefore the same flux density components without fault.

The model of a faulty winding is presented in Fig. 4 where the whole phase winding is composed of an elementary healthy section and one with short circuit turns. Therefore, the resulting air-gap flux density b^* of the faulty machine is equal to the initial one, *b*, which is added to the flux density b_{sc} generated by the y turns flowing through by the current i^s_{qsc} : $b^* = b + b_{sc}$ is added.

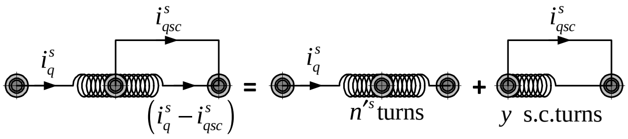

Fig. 4. Modelling of a faulty winding

The short circuit current is defined as follows:

$$i^s_{qsc} = I^s_{sc}\sqrt{2}\cos(\omega t - \varphi_{sc})$$

φ_{sc} is the phase lag between the short circuit current and the phase 1 current. This phase actually depends on several parameters such as the impedance that limits the short circuit current; the short circuit winding, and the position of the fundamental air-gap flux density relatively to the phase q current (depending on the load).

2.2. FAULTY TURNS MMF

The magneto motive force ε^s_{qsc} generated by the y short circuit turns, shifted of α^s_q from d^s, is shown in Fig. 5 in the case of a 4 pole machine. It also shows the mmf ε^s_{qel} generated by the healthy elementary winding. ε^s_{qsc} is an unidirectional mmf and can be decomposed in rotating fields which rotate in opposite directions. In a stator referential, ε^s_{qsc} can be written as follows:

$$\varepsilon^s_{qsc} = I^s_{sc} \sum_h A'^s_h \cos(\omega t - h\alpha^s - \varphi_h)$$

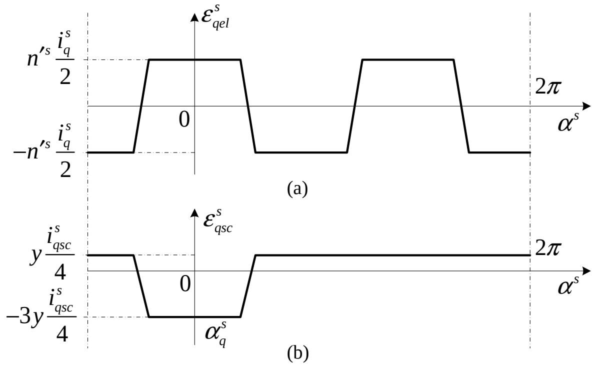

ig. 5. Mmf generated by the faulty turns.

A'^s_h is a function that can be determined from the Fourier series of ε^s_{qsc} and h is a non-null relative integer, which can take consequently all the values of h^s. φ_h is defined as: $\varphi_h = h\alpha^s_q + \varphi_{sc}$.

As $b_{sc} = \lambda\varepsilon^s_{qsc}$, the calculus developments lead to define this quantity in the reference frame related to d^s. After regrouping the components of same frequency and same polarity, it comes:

$$b_{sc} = \sum_{K_{sc},H_{sc}} \hat{b}_{sc\,K_{sc},H_{sc}} \cos\,(K_{sc}\omega t - H_{sc}\alpha^{s} - \varphi_{sc,K_{sc},H_{sc}})$$

with:

$$\left.\begin{aligned} K_{sc} &= 1+2kr' \\ H_{sc} &= h+p(ks'N^{s}+2kr') \end{aligned}\right\} \qquad (2)$$

ks' and *kr'* are equivalent to *ks* and *kr*, they vary from -∞ to + ∞. The resultant flux density appears, after attenuation, at the level of the external transverse field. One can also define $b^{x}_{sc,K_{sc}}$, the harmonic of K rank at the point M', of magnitude $\hat{b}^{x}_{sc,K_{sc}}$:

$$\bar{b}^{\,x}_{sc,K_{sc}} = \hat{b}^{\,x}_{sc,K_{sc}} \cos\,(K_{sc}\omega t - \varphi^{x}_{sc,K_{sc}})$$

$$\hat{b}^{\,x}_{sc,K_{sc}} = \left| \sum_{H} C_{H}\, \hat{b}_{sc,K_{sc},H_{sc}}\, e^{-j(H\alpha_{0}^{s}+\varphi_{sc,K_{sc},H_{sc}})} \right|$$

Considering the values that can be taken by K given by (1) and K_{sc} by (2), it results that K_{sc} does not bring new frequencies. That means that with the traditional method of diagnosis, the failure presence will be appreciated through the variation of the amplitudes of already existing lines in the spectrum. This makes the diagnosis by analysis of the changes in the amplitudes of the measured components difficult.

According to the values taken by K_{sc}, it appears that the sensitive harmonics are in low frequency. Indeed, the corresponding harmonics, for k'r=±1, are at 50Hz and 150Hz. Consequently, as one of these components is confused with the fundamental, the harmonic at 150Hz will be analysed for the diagnosis.

2.3. VARIATION OF OPERATING CONDITIONS.

Only the sensitive components $\mathrm{b}^{\mathrm{x}}_{\mathrm{sc,K_{sc}}}$ at 150Hz defined in the previous section is now considered: $\mathrm{b}^{\mathrm{x}}_{\mathrm{sc,K_{sc}}}$ merge with b^{x}_{K} relative to the healthy machine to generate the resulting harmonic flux density b^{*x}_{K}. Actually when operating condition changes, b^{x}_{K} and the phase lags φ_{sc}, φ_{h} change, but it will be assumed that $\mathrm{b}^{\mathrm{x}}_{\mathrm{sc,K_{sc}}}$ does not change. Consequently, for position 1 (sensor 1) defined for $\alpha^{s}=0$, and position 2 (sensor 2) defined for $\alpha^{s}=\pi$, the resulting harmonic b^{*x}_{K} can be expressed as follows:

Sensor 1 :

$$b^{*x1}_{K} = \hat{b}^{\,x}_{K} \cos\,(K\omega t - \varphi^{x}_{K}) + \hat{b}^{\,x}_{sc,K_{sc}} \cos\,(K_{sc}\omega t - \varphi^{x}_{sc,K_{sc}})$$

Sensor 2 :

$$b^{*x2}_{K} = \hat{b}^{\,x}_{K} \cos\,(K\omega t - \varphi^{x}_{K}) - \hat{b}^{\,x}_{sc,K_{sc}} \cos\,(K_{sc}\omega t - \varphi^{x}_{sc,K_{sc}})$$

The only change between sensor 1 and sensor 2 is the change of the sign of the faulty term. This is due to the polarity $H_{sc}=1$ that changes the sign of the cosinus (cos(γ+π)=-cos(γ)), whereas to polarity H=2 of the healthy term does not change the sign: cos(γ+2π)=cos(γ). In a physical point of view, the dissymmetry generated by the fault is the base of the property.

Fig. 6a gives the associated time phasor diagram for $\varphi^{x}_{K}=0$. The Figure clearly shows that the magnitudes of the complex quantities $\bar{b}^{*x1}_{K}$ and $\bar{b}^{*x2}_{K}$ are different. Fig.6b gives the time phasor diagram after a variation of operating condition. It can be observed that the resulting magnitudes $\hat{b}^{*x1}_{K}$ and $\hat{b}^{*x2}_{K}$ do not evolve in similar way.

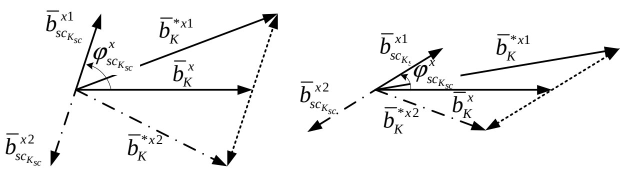

(a) operating condition 1 (b) operating condition 2

Fig. 6. Phasor diagram variation

The property tied to the variation of the magnitude $\hat{b}^{*x}_{K}$ allows one to propose a diagnosis method based on the following properties:

- *In healthy conditions:*

The term $b^{x}_{sc,K_{sc}}$ is null and when operating condition changes, the air-gap flux density stays practically identical. As the external elements responsible for the attenuation act in the same way in positions 1 and 2 for the no-load and for the load tests, the amplitudes $\hat{b}^{*x1}_{K}$ and $\hat{b}^{*x2}_{K}$ keep similar values or at least evolve in the same way when the machine is loaded.

- *In faulty conditions:*

In case of variation of operating conditions, the magnitude of the component at $K\omega$ angular frequency measured in positions 1 and 2 will not evolve similarly. The variations of the harmonic at $K\omega$ are thus an indicator of a defect.

The advantage of the method is that it does not require the knowledge of the presumed healthy state to detect the fault.

In the case of a generator connected to the grid, the operating condition of the synchronous machine can be the active power P or the reactive power Q delivered to the grid.

3. EXPERIMENTAL ANALYSIS

3.1. TEST BENCH DESCRIPTION

Tests have been done on a salient-pole synchronous machine characterized by: 7.5kW, p=2, N^s=18, 50Hz, 230/400V.

To make the tests, the machine has been rewound to allow a direct access of the terminals of the stator elementary sections. The machine with sensors placed at 180° from each other around the frame is shown in Fig. 7.

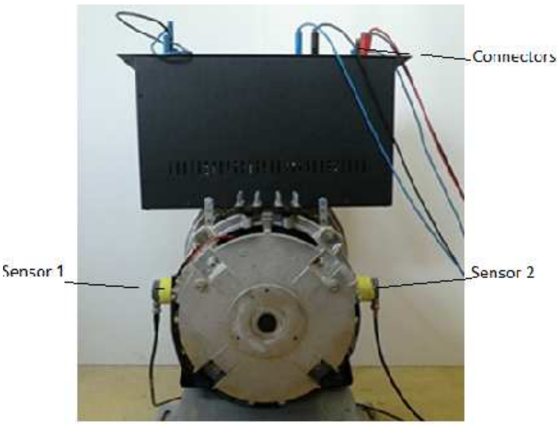

Fig. 7, the synchronous machine and the flux sensors

In power plants it is generally more easy to make variations of reactive power than active power. Actually reactive power can simply be changed through field excitation current, whereas active power variations required to act on the mechanical system associated to the generator.

3.2. RESULTS

Tests have been done at two active power: at no load (P=0) and at third to rated power (P=2500W), and for two faulty mode: in heathy condition and with a short circuit of half of the wires placed in one slot , what corresponds to 8.5% of one phase winding. The short circuit current is limited to 15A rms.

Fig. 8 gives the harmonic at 150Hz computed from the signal delivered by the both sensors (S1 and S2) versus the reactive power for P=0, in healthy and faulty conditions. Fig. 9 gives the same information but for P=2500W.

Results that were predicted theoretically are verified experimentally. For the healthy machine (Fig. 8.a and Fig. 9.a), it can be observed that the variations of the harmonic at 150Hz are similar. In faulty case (Fig. 8.b and Fig. 9.b) these variations are different, especially in loaded conditions (Fig. 9). It can be also observed that the difference of variations is more importance when the machine receive reactive power from the grid (Q<0).

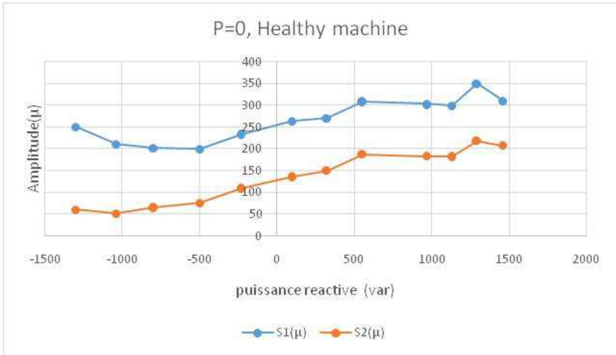

(a) healthy machine

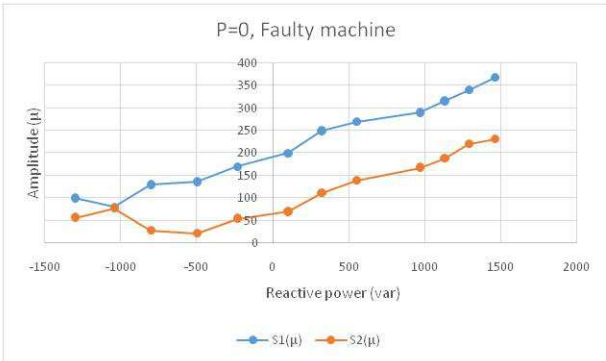

(b) faulty machine

Fig. 8 – 150Hz harmonic at no load

3.3. DISCUSSION

The proposed methods has the main advantage of being fully non invasive, simple to implement and it is not based on a comparison of the actual state with a previous healthy state. However, it requires to make changes of the operating conditions of the machine. The method has also some limitations. Firstly, as highlighted in analytical developments, it should be pointed out that the method cannot be applied to 2-pole machines as it is based on the difference between electrical and geometrical positions. Secondly, it has been shown in [11] that the difference of variation between the both sensors depends on the position of the sensors relatively to the faulty winding. Therefore, in order to increase the reliability of the methods, measurements at several positions are advised.

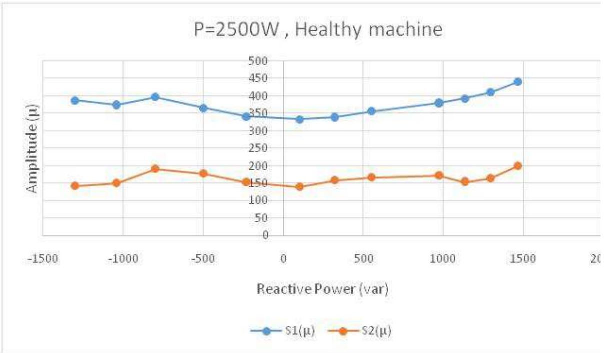

(a) healthy machine

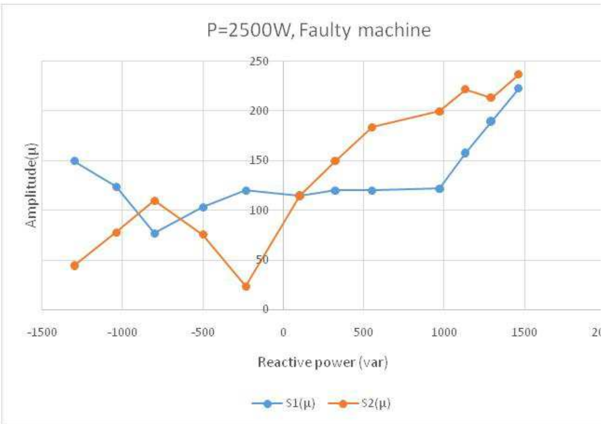

(b) faulty machine

Fig. 9 – 150Hz harmonic with active power sent to the grid

CONCLUSION

The work presented in this paper concerns a procedure for detection of inter-turn short circuits in the stator windings of a synchronous generator. This procedure uses the information available in the external magnetic field measured by two flux sensors placed against the machine, which respect a specific position and an angular shift. This procedure is non-invasive and inexpensive, characterized by the exploitation of the spatial dissymmetry of the external magnetic field in the vicinity of the machine. Actually, the procedure exploits the variation of sensitive spectral lines extract from the signal when the reactive power varies. The advantage is that the reactive power can be simply changes through the rotor field current. The obtained results show that it is not necessary to know a presumed healthy state to proceed to the diagnostic. Further work consists in extracting features from the signal to make a decision concerning the presence of a fault.

REFERENCES

[1] W.Q. Lim, D.H. Zhang, J.H. Zhou, P.H. Belgi, H.L. Chan, “Vibration-based fault Diagnosis platform for rotary machines”, *36th Annual Conference on IEEE Industrial Electronics Society (IECON 2010)*, pp. 1404 – 1409, 2010

[2] H. Henao, H. Razik, and G. A. Capolino, “Analytical approach of the stator current frequency harmonics computation for detection of induction machine rotor faults,” *IEEE Trans. Ind. Appl.*, vol. 41, no. 3, pp. 801–807, May/Jun. 2005

[3] W. T. Thomson and M. Fenger, “Current signature analysis to detect induction motor faults,” *IEEE Ind. Appl. Mag.*, vol. 7, no. 4, pp. 26–34, Jul./Aug. 2001.

[4] S. Nandi, H. A. Toliyat, and L. Xiaodong, “Condition monitoring and fault diagnosis of electrical motors—A review,” *IEEE Trans. Energy Convers.*, vol. 20, no. 4, pp. 719–729, Dec. 2005.

[5] P.J. Tavner, P. Hammond, J. Penman, “Contribution to the study of leakage fields at the ends of rotating electrical machines”, IEE, Vol. 125, N°12, 1978, pp.1339-1349.

[6] L. Frosini, A. Borin, L. Girometta, G. Venchi, “A novel approach to detect short circuits in low voltage induction motor by stray flux measurement”, *20th International Conference on Electrical Machines (ICEM ’12)*, pp. 1536 – 1542, Sept. 2012.

[7] R. Romary, R. Corton, D. Thailly, and J. F. Brudny, "Induction machine fault diagnosis using an external radial flux sensor", *The European Physical Journal - Applied Physics*, vol. 32, pp. 125-132, 2005.

[8] A. Ceban, R. Pusca, and R. Romary, “Study of rotor faults in induction motors using external magnetic field analysis,” *IEEE Trans. Ind. Electron.*, vol. 59, pp. 2082-2093, May 2012.

[9] R. Pusca, R. Romary, A. Ceban, and J.-F. Brudny, "An Online Universal Diagnosis Procedure Using Two External Flux Sensors Applied to the AC Electrical Rotating Machines," *Sensors*,vol. 10, 2010, pp. 10448-10466.

[10] D. Thailly, R. Romary, D. Roger, J.F. Brudny, “Attenuation of magnetic field components through an AC machine stator”. COMPEL, Vol. 27, No. 4, 2008, pp.744-753.

[11]R. Pusca, C. Demian, D. Mercier, E. Lefevre, R. Romary “Improvement of a diagnosis procedure for AC machines using two external flux sensors based on a fusion process with belief functions”, *IECON2012*, 25-28 October 2012, Montreal, Canada, pp. 5078-5083.